

## Synthesis and Characterization of ZnO/MnFe<sub>2</sub>O<sub>4</sub> Nanocomposites for Degrading Cationic Dyes

Yuniar<sup>1</sup>, Tuty Emilia Agustina<sup>2\*</sup>, Muhammad Faizal<sup>2</sup>, Poedji Loekitowati Hariani<sup>3</sup>

<sup>1</sup> Doctoral Program of Engineering Science, Chemical Engineering Department, Universitas Sriwijaya, Jalan Srijaya Negara, Bukit Besar, Palembang 30139, South Sumatera, Indonesia

<sup>1</sup> Department of Chemical Engineering, Politeknik Negeri Sriwijaya, Jalan Srijaya Negara, Bukit Besar, Palembang, 30139, South Sumatera, Indonesia

<sup>2</sup> Department of Chemical Engineering, Faculty of Engineering, Universitas Sriwijaya, Jalan Palembang-Prabumulih Km 32, Indralaya, Ogan Ilir 30662, South Sumatera, Indonesia

<sup>3</sup> Department of Chemistry, Faculty of Mathematics and Natural Sciences, Universitas Sriwijaya, Jalan Palembang-Prabumulih Km 32, Indralaya, Ogan Ilir 30662, South Sumatera, Indonesia

\* Corresponding author's e-mail: tuty\_agustina@unsri.ac.id

### ABSTRACT

By breaking down harmful dye waste into harmless components under the right irradiation sources, photocatalysis is an unorthodox but promising technique that can reduce industrial wastewater pollution, particularly in the textile industry. Synthetic textile dyes called cationic dyes must be handled carefully because they are poisonous and challenging to breakdown. Photocatalytic oxidation is a useful technique for eliminating hazardous organic pigments. This investigation aims to synthesize and characterize ZnO/MnFe<sub>2</sub>O<sub>4</sub> nanocomposites as well as investigate the effects of varying ZnO:MnFe<sub>2</sub>O<sub>4</sub> ratios, pH levels, doses, and irradiation times on band gap reduction and photocatalytic applications tested with cationic dyes, specifically methylene blue, under the illumination of sunlight. The co-precipitation approach for the manufacture of nanocomposites with different mole ratios of ZnO:MnFe<sub>2</sub>O<sub>4</sub> (1:0.1; 2:0.1; 3:0.1). The component comprising the nanocomposite is ZnO/MnFe<sub>2</sub>O<sub>4</sub>, according to the results of the characterisation using XRD, SEM-EDX, FTIR, and BET. UV-DRS measurements of the band gap revealed that as ZnO was reduced, the band gap of the nanocomposite likewise decreased, from 3.35 eV to 2.78 eV. The greatest degradation of 93.2% was achieved for the degradation of 50 mg/L methylene blue (MB) dye with a catalyst dosage of 20 mg at a ratio of 1:0.2 for 50 minutes of irradiation. Since the point of zero charges (pzc) was reached at a pH of 7.8, a photodegradation adsorption-friendly solution pH of 8 was created.

**Keywords:** nanocomposite, ZnO/Fe<sub>2</sub>O<sub>4</sub>, cationic dyestuff, photocatalytic.

### INTRODUCTION

The growth of textile industry sector in Indonesia is growing rapidly so it has a positive impact on human life. However, in addition to having a positive impact, it also has a negative impact on the environment because it produces waste that contains large amounts of dye. Wastewater containing pollutants in the form of dyes from textile wastewater has many major problems, namely negative impacts such as carcinogenic, causing allergies, skin irritation, and others. Pollutants in the form of dyes were found to be very resistant

to biological, physical, and chemical reactions (Wang et al., 2015). Most of the dyes used in the dyeing process in the textile industry will be wasted in the environment as waste. Textile industry wastewater contains organic compounds with high enough concentrations in almost every process unit. As a result, the water quality decreases because it is mixed with wastewater. Due to their large molecular weight and biochemical durability, dyes from manufactured wastewater are organic molecules with an aromatic structure that are difficult to break down naturally and are not environmentally friendly. The removal of these

harmful organic wastes by conventional methods such chemical, physical, and biological processes is exceedingly challenging.

Methylene blue dye is a toxic aromatic hydrocarbon compound including cationic dyes with very strong adsorption power (Długosz et al., 2020). Based on the effect caused by the dye on the environment, it is necessary to make various efforts to minimize the dye waste before being discharged into the waters.

Various methods such as chemical filtration, coagulation, electrocoagulation, and adsorption have been applied to remove textile dye waste. However, these methods are less effective in dealing with textile dye waste, so they will create new problems for the environment (Gómez-pastora et al., 2017). To overcome this, several studies have been carried out on wastewater treatment. Of the several ways that can be done, the use of photocatalysts is one of the most effective ways of treating wastewater. In the process of converting light energy into chemical energy, photocatalysts create hydroxyl radicals, which redox react with organic contaminants to restore the clarity of the water by separating it from wastewater. These contaminants are transformed into more environmentally friendly  $O_2$  and  $H_2$  (Mano et al., 2015; Wang et al., 2015). A photocatalyst is used in the photodegradation process to break down the procion red dye (Agustina et al., 2020). Anionic and cationic dye organic pollutants are degraded by nanocomposite  $Fe_3O_4/ZnO$  photocatalysis (Długosz et al., 2020).

Nanocomposite  $Fe_3O_4/ZnO$  photocatalysis is used to degrade organic pollutants in the form of anionic and cationic dyes (Długosz et al., 2020).

Zinc oxide is an environmentally friendly material without affecting the life of organisms, human health, and the environment. In comparison to other metal-oxide semiconductors, ZnO has a wide band gap, a near UV spectral area, is highly effective at removing and fully degrading dyes, and has the ability to absorb a wide range of solar radiation (Gayatri et al., 2020; Ong et al., 2018). The ZnO photocatalyst technique, however, primarily utilizes UV light sources since the ZnO band gap energy is relatively big, measuring 3.37 eV, making it less efficient when using sunlight because it only employs 5% of the sunshine spectrum (UV fraction of sunlight) (Zhang et al., 2016).

The constraints of employing ZnO to degrade organic pollutants, particularly dyes, will be eliminated by modification of the ZnO photocatalyst

mixed with  $MnFe_2O_4$ , which may be activated using visible light. For the redox potential scale of 1.47 eV, manganese ferrite ( $MnFe_2O_4$ ) has a low band gap energy, conduction band (CB), and valence band (VB). (Chandel et al., 2020; Kefeni & Mamba, 2020). This can reduce the ZnO band gap so that the degradation process using a ZnO/ $MnFe_2O_4$  photocatalyst can use sunlight as a source. Manganese ferrite has magnetic permeability properties, high chemical stability, and good catalytic properties. Combined ZnO/ $MnFe_2O_4$  will improve the performance of the semiconductor. Manganese ferrite which is magnetic can facilitate the separation so that the combined ZnO/ $MnFe_2O_4$  using external magnets and photocatalysts can be used repeatedly (Kefeni & Mamba, 2020).

The co-precipitation process is one of the most effective ways to create nanocomposites. As a result, this technique can be used to create ZnO/ $MnFe_2O_4$  nanocomposite materials. Manganese ferrite, one of the nanomagnetic nanoparticles, is frequently utilized in adsorption, catalysis, and environmental investigation (Rahmayeni et al., 2017).

In this study, the co-precipitation method was used to investigate the degradation of methylene blue dye in order to characterize and synthesize ZnO/ $MnFe_2O_4$  nanocomposite for photocatalysis.

## MATERIALS

In this study, the following chemicals were used: Zinc chloride (CAS No. 7646-85-7, purity 99.99%), Sodium hydroxide (CAS No. 1310-73-2, 50% purity in water), Iron (III) chloride hexahydrate (CAS No. 10025-77-1, purity 97%), Manganese (II) chloride tetrahydrate (CAS No. 13446-34-9, 99% purity), Polyethylene glycol (PEG) (CAS No. 25322-68-3), Methylene blue (61-73-4), Absolute ethanol (CAS No. 64-17-5, purity 99.5%), deionized water and distillate water.

### Material characterization

X-Ray diffraction (XRD), scanning electron microscope-energy dispersive X-ray (SEM-EDX), and fourier transform infrared were used to evaluate ZnO/ $MnFe_2O_4$  nanocomposites. SEM-EDX analysis was done to examine the morphology or surface image of the material, and XRD analysis was done to see the crystal structure based on the scattering angle peak information

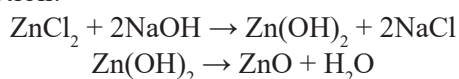
(XRD Rigaku MiniFlex 600). (SEM-EDX Tescan vega 3),

FTIR was performed to determine the functional group (FTIR Thermo Nicolet iS10). To observe the surface area using Brunauer, Emmett, and Teller (BET Phenom Pro X Desktop SEM) and Analysis of the determination of band gap energy using a Diffuse Reflectance UV Vis spectrophotometer (DR UV Vis brand Shimadzu UV-2401 PC).

## METHODS

### Production of ZnO nanoparticles

Pure ZnO nanoparticles (NP) were synthesized using the direct precipitation method. Solutions of 1 M ZnCl<sub>2</sub> and 2 M NaOH were prepared separately by dissolving them in deionized water. The NaOH solution was added dropwise into the ZnCl<sub>2</sub> solution until it reached pH solution 12 and stirred constantly using a magnetic stirrer at 400 rpm for 2 hours at room temperature to form a white suspension. Centrifugation at 5000 rpm for 15 minutes separated the white precipitate from the solution after two hours of stirring. The product was then rinsed again with absolute ethanol and deionized water until the pH was neutral. After that, ZnO was created by calcining the white precipitate in a furnace for two hours at 500 °C. Reaction:

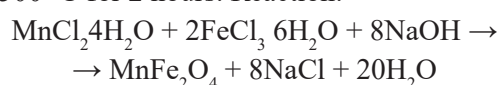


### Synthesis of MnFe<sub>2</sub>O<sub>4</sub>

MnFe<sub>2</sub>O<sub>4</sub> nanoparticles were prepared using the co-precipitation method by mixing MnCl<sub>2</sub>·4H<sub>2</sub>O and FeCl<sub>3</sub>·6H<sub>2</sub>O as providers of Mn<sup>2+</sup> and Fe<sup>3+</sup> ions with a reaction coefficient ratio of 1:2. Solutions of 0.2 M MnCl<sub>2</sub>·4H<sub>2</sub>O and 0.4 M FeCl<sub>3</sub>·6H<sub>2</sub>O were prepared using deionized water, respectively. With the same volume, the two solutions were mixed and stirred rapidly using a magnetic stirrer for 1 hour at 80 °C. The solution was added with 2 M NaOH dropwise until it reached pH 12 and a brown precipitate was formed.

The precipitate was separated with a permanent magnet and washed with deionized water until the pH was neutral, followed by absolute alcohol, and dried in an oven at 70 °C for 4 hours.

The dried MnFe<sub>2</sub>O<sub>4</sub> nanoparticles were ground and sieved with a size of 200 mesh. Furthermore, it is calcined in a furnace at a temperature of 500 °C for 2 hours. Reaction:



### Synthesis of ZnO/MnFe<sub>2</sub>O<sub>4</sub> nanocomposites

Various ZnO:MnFe<sub>2</sub>O<sub>4</sub> ratios were used to prepare the ZnO/MnFe<sub>2</sub>O<sub>4</sub> synthesis (1:0.1; 2 0.1 and 3:0.1). In 50 ml of distilled water, 2 g of ZnO and 1 g of PEG 4000 were combined and agitated at 500 rpm for an hour at 80 °C. The ZnO-PEG combination was then added, and 1.335 g of FeCl<sub>3</sub>·6H<sub>2</sub>O and 0.488 g of MnCl<sub>2</sub>·H<sub>2</sub>O were weighed, dissolved in 50 ml of distillate water, and added. This mixture was then agitated for an hour while remaining at 80 °C with drops of 2 M NaOH until it reached pH solution 12.

The precipitate was separated with a permanent magnet and washed with deionized water until the pH was neutral, followed by absolute alcohol, and dried in an oven at 70 °C for 4 hours. The dried MnFe<sub>2</sub>O<sub>4</sub> nanoparticles were ground and sieved with a size of 200 mesh.

After washing the precipitate with deionized water until the pH was neutral, absolute ethanol was applied. The precipitate was dried for eight hours in an oven at 80 °C. In addition, it is calcined in a furnace for two hours at 500 °C to create ZnO/MnFe<sub>2</sub>O<sub>4</sub>. Furthermore, XRD, BET, SEM-EDX, FTIR, and UV-DRS were used to characterize it.

### Determination of pH point zero charge (pHpzc)

A change to the method is called “determination of pH pzc” (Kulkarni et al., 2017). To each of the 11 Erlenmeyer, a total of 30 mL of a 5 mM NaCl solution was added. By adding a solution of 0.1 M HCl or 0.1 M NaOH, the solution’s initial pH was changed from 2-12. Each Erlenmeyer was then filled with 0.23 g of the photocatalyst, and it was agitated for an hour with a magnetic stirrer. A pH meter was used to determine the final pH of each solution after the mixture was let to stand for 48 hours.

## Photocatalytic degradation test

The photocatalytic activity of ZnO/MnFe<sub>2</sub>O<sub>4</sub> nanocomposite with a mole ratio of ZnO: MnFe<sub>2</sub>O<sub>4</sub> is 1:0.1; 2:0.1 and 3:0.1 were evaluated by measuring the photocatalytic degradation of methylene blue with a concentration of 50 ppm for 50 minutes with a catalyst dose of 20 mg. From the three nanocomposites, one nanocomposite will be obtained that can degrade certain MB dyes.

The degradation of methylene blue synthetic dyes was used to investigate the photocatalytic activity of ZnO/ MnFe<sub>2</sub>O<sub>4</sub> nanocomposites. A 10W Philips LED bulb was used in the reactor for the photocatalytic test. The ZnO/ MnFe<sub>2</sub>O<sub>4</sub> nanocomposite was weighed up to 20 mg, and 50 ml of synthetic methylene blue dye with a concentration of 50 ppm was added. At room temperature, the mixture was continuously stirred using a 400-rpm magnetic stirrer. To measure the color degradation, samples are taken every 10, 20, 30, 40, and 50 minutes starting when the lamp is turned on.

The experiment was repeated while keeping the concentration of the dye solution at 50 ppm and using various catalyst doses of 5, 10, 15, 20, and 25 mg. After the allotted amount of time has passed, the sample is taken, and the catalyst is then removed from the solution using a Whatman filter. To determine the percentage of methylene blue degradation, the solution's absorbance was measured using a UV-Vis spectrophotometer at a wavelength of 588 nm. ZnO, MnFe<sub>2</sub>O<sub>4</sub>, ZMn-1,

ZMn-2, and ZMn-3 underwent the same treatment. The quantity of methylene blue and the percentage of photodegradation of methylene blue were both determined from this absorbance value.

$$\text{Degradation (\%)} = [(Co-C)/Co] \times 100\% \quad (1)$$

The formula to get the percentage of dye degradation is shown in equation (1), where Co and C represent the solution's initial and post-degradation concentrations, respectively.

## RESULTS AND DISCUSSION

### ZnO/MnFe<sub>2</sub>O<sub>4</sub> nanocomposite characterization results

#### Structural analysis

The structure and particle size of the resulting sample were analyzed by X-ray diffractometer (Rigaku MiniFlex 600 XRD Analytical). XRD patterns of ZnO, MnFe<sub>2</sub>O<sub>4</sub> nanoparticles, and nanocomposites with variations in the ratio of ZnO: MnFe<sub>2</sub>O<sub>4</sub> synthesized by the co-precipitation method are shown in Figure 1.

Sample values were found at  $2\theta = 31.78$  (hkl 100), 34.42 (hkl 002), 36.25 (hkl 101), 47.54 (hkl 102), 56.60 (hkl 110), 62.86 (hkl 103), 66.38 (hkl 200), 67.96 (hkl 112), 69.10 (hkl 201), 72.56 (hkl 004), and 76.96 (hkl 202). This peak demonstrated that ZnO nanoparticles formed in the hexagonal wurtzite crystal structure. This peak

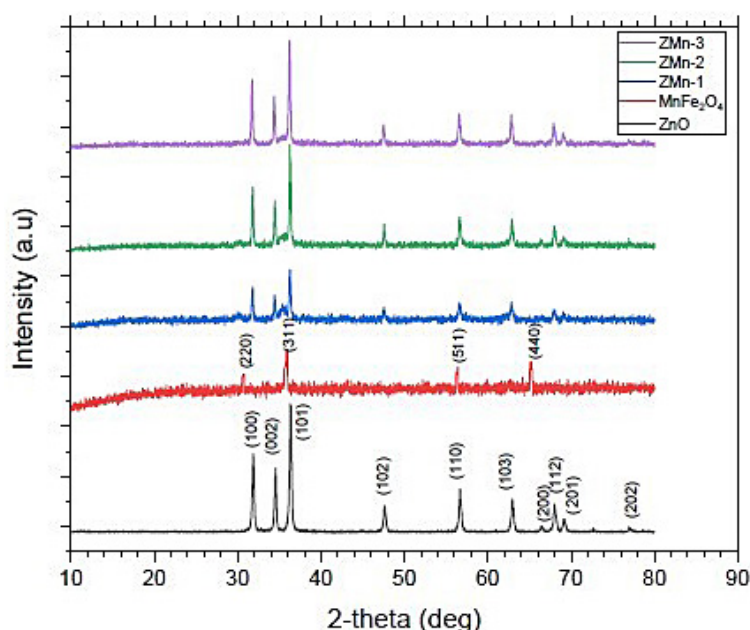


Figure 1. XRD of ZnO/MnFe<sub>2</sub>O<sub>4</sub> photocatalyst

matches the JCPDS No. 00-36-1451 hexagonal ZnO standard XRD data table. According to the spinel cube structure of JCPDS No. 00-73-1964, the diffraction peaks for the  $\text{MnFe}_2\text{O}_4$  sample were detected at  $2\theta = 29.90$  (hkl 220),  $35.17$  (hkl 311),  $56.5$  (hkl 511), and  $62.27$  (hkl 440).

This peak confirmed the formation of the hexagonal wurtzite crystal structure of ZnO nanoparticles. This peak corresponds to the hexagonal ZnO standard XRD data table of JCPDS No. 00-36-1451. For the  $\text{MnFe}_2\text{O}_4$  sample, the diffraction peaks with sample values were observed at  $2\theta = 29.90$  (hkl 220),  $35.17$  (hkl 311),  $56.5$  (hkl 511),  $62.27$  (hkl 440) according to the spinel cube structure of JCPDS No. 00-73-1964. The XRD pattern of ZMn nanocomposites with variations in the composition of ZnO (ZMn-1, ZMn-2, and ZMn-3) showed that the peak was dominated by ZnO with a wurtzite structure. It also showed that the addition of ZnO did not change the structure of  $\text{MnFe}_2\text{O}_4$  in the nanocomposite, because the amount of  $\text{MnFe}_2\text{O}_4$  was small and the crystallinity was low, ZMn-1 did not exhibit the primary diffraction peak  $2\theta = 35.17$  (hkl 311). The primary peaks of ZnO emerged as the amount of ZnO in the nanocomposite grew, as illustrated in ZMn-2 and ZMn-3. No further peaks were seen in any of the ZMn nanocomposite XRD patterns, showing the material was free of contaminants.

Using the Debye-Scherrer formula, the crystal size of ZnO nanoparticles in nanocomposites can be determined from the highest peak (Kaur et al., 2013). ZnO and  $\text{MnFe}_2\text{O}_4$  nanoparticles had crystal diameters of 26.87 nm and 1.65 nm, respectively, whereas ZMn-1, ZMn-2, and ZMn-3 nanocomposites had sizes of 26.49, 43.71, and 39.57 nm. This suggests that the resulting ZnO/ $\text{MnFe}_2\text{O}_4$  composite has achieved nano size, leading to the conclusion that the co-precipitation process used to create the ZnO/ $\text{MnFe}_2\text{O}_4$  nanocomposite was successful.

### Morphological analysis and elemental composition

Scanning electron microscopy (SEM) was used to examine the materials' morphology (SEM Tescan Vega 3). Figure 2 displays the surface morphology of ZnO,  $\text{MnFe}_2\text{O}_4$ , ZMn-1, ZMn-2, and ZMn-3 with variations in ZnO content. ZnO has a uniform shape (Figure 2a) and evenly scattered granules with an average particle diameter of 26.87 nm. While agglomeration

and non-homogeneous shape of the  $\text{MnFe}_2\text{O}_4$  nanoparticles (Figure 2b) were evident. ZMn-1, ZMn-2, and ZMn-3 nanocomposites' morphology Figure 2c-e demonstrates the existence of two distinct component types in the nanocomposite.

The attachment of  $\text{MnFe}_2\text{O}_4$  particles to the ZnO surface, as well as the color combination of the light-colored ZnO and the dark-colored  $\text{MnFe}_2\text{O}_4$ , were distinguishing features of the SEM morphological study results.

The composition of the elements in the nanoparticles and nanocomposites obtained from EDX as shown in Table 1. EDX results of elements contained in nanoparticles and nanocomposites before and after being combined. From the results of EDX characterization, the chemical content in ZnO and  $\text{MnFe}_2\text{O}_4$  nanoparticles before being combined, for ZnO is 73.37% Zn and 26.63% O while for  $\text{MnFe}_2\text{O}_4$  is 4.19% O, 95.74% Fe and 0.07% Mn. Only Zn, O, Fe, and Mn elements are present in the nanocomposite, according to the elemental composition determined by EDX. Zn's additional peak in the EDX results from a significant amount of ZnO adhering to  $\text{MnFe}_2\text{O}_4$  nanoparticles. Table 1 shows the proportions of Zn, Mn, Fe, and O in ZMn-1, ZMn-2, and ZMn-3. This demonstrated that the processed samples were pure and free of any extraneous contaminants.

### Functional group analysis

The primary functional groups in the substance were identified using FTIR analysis. Figure 3 shows the FTIR spectra of ZnO,  $\text{MnFe}_2\text{O}_4$ , ZMn-1, ZMn-2, and ZMn-3. As demonstrated in Figure 3, the Zn-O strain vibration can be attributed to the ZnO nanoparticle band at  $445\text{ cm}^{-1}$ . The existence of  $\text{MnFe}_2\text{O}_4$  is indicated by the band seen at  $556\text{ cm}^{-1}$  in  $\text{MnFe}_2\text{O}_4$  nanoparticles, which correlates to the creation of metal-oxygen stretching vibrations (Shoueir et al., 2018). The spectrum of the ZnO/ $\text{MnFe}_2\text{O}_4$  nanocomposite photocatalyst heterogeneous system confirms the presence of ZnO and  $\text{MnFe}_2\text{O}_4$  as shown in Figure 3.

At  $3431\text{ cm}^{-1}$ , the water adsorbed on the nanocomposite surface generated the OH stretching vibration that was detected. The stretching vibration of the MB bond at the spinel ferrite tetrahedral site is linked to the absorption band at  $579\text{ cm}^{-1}$ . Water molecules are physically adsorbed onto the surface of the nanoparticles, causing

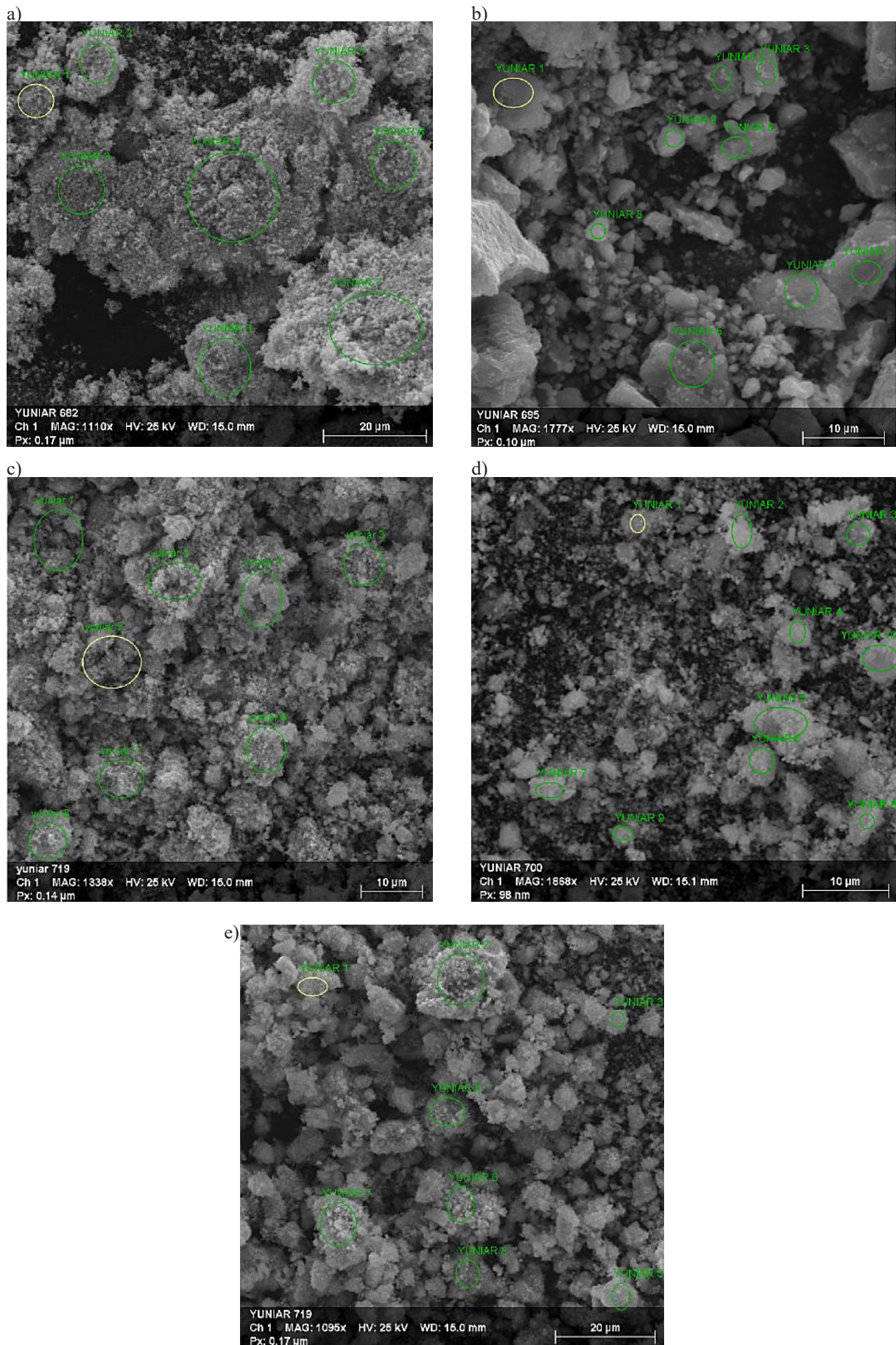
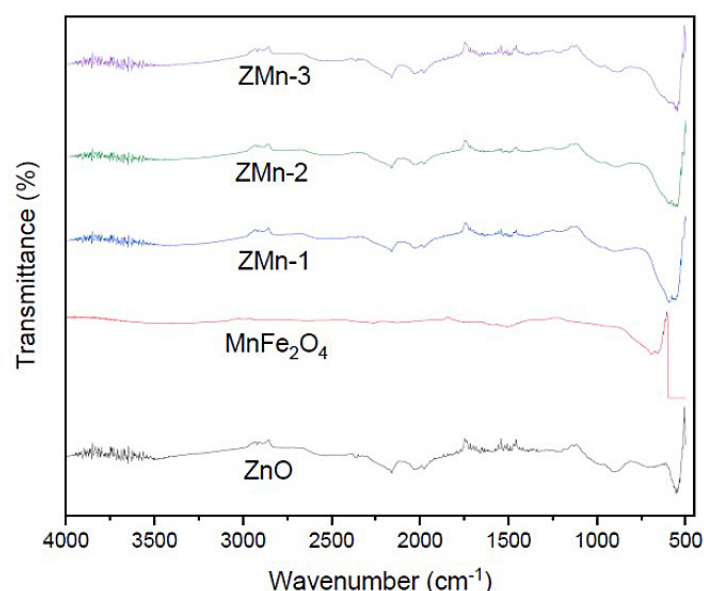


Figure 2. SEM Analysis of (a) ZnO; (b) MnFe<sub>2</sub>O<sub>4</sub>; (c) ZMn-1; (d) ZMn-2; (e) ZMn-3

**Table 1.** Results of EDX Analysis

Component	Weight percentage (%)				
	Nanoparticle of ZnO	Nanoparticle of $\text{MnFe}_2\text{O}_4$	ZMn-1 nanocomposite	ZMn-2 nanocomposite	ZMn-3 nanocomposite
Zn	73.37	-	79.21	52.73	53.21
O	26.63	4.19	14.77	34.06	24.64
Fe	0.00	95.74	5.96	8.78	15.94
Mn	0.00	0.07	0.06	4.43	6.21

**Figure 3.** FTIR Analysis of ZnO,  $\text{MnFe}_2\text{O}_4$ , ZMn-1, ZMn-2, and ZMn-3

O-H stretching vibrations that result in a bandwidth between 3600 and 3300  $\text{cm}^{-1}$  centered at 3420  $\text{cm}^{-1}$ .

The obtained samples were subjected to UV-Vis DRS analysis to ascertain the optical characteristics. The UV-Vis 2450 diffusion reflection spectra of  $\text{MnFe}_2\text{O}_4$  and nanocomposites are displayed in Table 2. The spectra of  $\text{MnFe}_2\text{O}_4$  exhibits strong absorption for pure ZnO below 400 nm and high adsorption intensity in the broad visible light range between 400 and 800 nm. ZMn-1, ZMn-2, and ZMn-3 had adsorption areas with their respective band gaps at wavelengths of 524-590, 509-895, and 513-879 nm, respectively (Table 2).

Using the Kubelka-Munk function and the equation  $F(R) = (1R)/2R$ , where R is the sample's diffuse reflectance, the band gap energy is computed (Boutra et al., 2020). A diffuse reflectance spectrum is used to calculate band gap energy according to Kubelka Munk's hypothesis. The band gap energies of ZnO,  $\text{MnFe}_2\text{O}_4$ , ZMn-1, ZMn-2, and ZMn-3 are displayed in Table 2.  $\text{MnFe}_2\text{O}_4$  has the lowest band gap, however despite

this, it is not a photocatalytically active material. The quick recombination of charge carriers can account for this. Because ZnO has a greater band gap than  $\text{MnFe}_2\text{O}_4$ , the band gap energy of  $\text{MnFe}_2\text{O}_4$  marginally increases with ZnO doping. Additionally, compared to the other samples, the band gap in nanocomposites with ZnO deposition on the surface is greater. Agglomeration in nanocomposites can be exacerbated by the energy level of the sub-band-gap created by surface and interfacial imperfections (Güy & Özacar, 2018).

The adsorption of UV light to the visible light region will rise in the nanocomposite by increasing ferrite and decreasing ZnO, it can be stated.

**Table 2.** Analysis result of surface area and band gap

Samples	Surface area ( $\text{m}^2/\text{g}$ )	Band gap (eV)
ZnO	3.359	3.35
$\text{MnFe}_2\text{O}_4$	71.108	1,8
ZMn-1	28.628	2.78
ZMn-2	19.296	3.19
ZMn-3	16.393	3.25

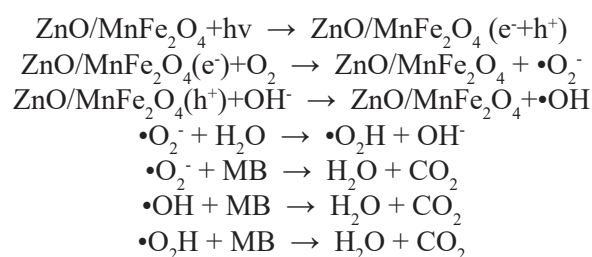
According to Table 2's BET values, ZnO has a surface area of 3.359 m<sup>2</sup>/g. ZnO nanoparticles have a smaller surface area than nanocomposites, while MnFe<sub>2</sub>O<sub>4</sub> nanoparticles have the largest surface area, namely 71.108 m<sup>2</sup>/g so that when composited the surface area decreases, this is due to the ratio of ZnO in nanocomposites which is greater than that of MnFe<sub>2</sub>O<sub>4</sub>. It can also be seen that the reduced MnFe<sub>2</sub>O<sub>4</sub> in the nanocomposite composition means the smaller the surface area per unit mass of the particles. This is because the greater the MnFe<sub>2</sub>O<sub>4</sub> in the particles, the more particles that agglomerate so that a lot of the surface area of the particles sticks to the surface area of other particles thereby reducing the surface area per unit mass of the particles.

The surface area can improve the desorption rate and adsorption capacity, which will have an effect on the degradation process. Particle sizes between 18 and 25 nm were produced when the surface area per unit mass of particles was converted to that of unagglomerated particles.

### Photocatalyst performance

Photocatalytic activity reduces dye contaminants in wastewater, adversely affecting the environment. The pollutant that will be degraded by ZnO/MnFe<sub>2</sub>O<sub>4</sub> nanocomposite is methylene blue. Figure 4 shows that ZnO/MnFe<sub>2</sub>O<sub>4</sub> exhibits different photocatalytic properties. The decrease in methylene blue with a concentration of 50 mg/L, catalyst dose of 0.02 mg/L under visible light irradiation after 50 minutes with ZMn-1, ZMn-2, ZMn-3 nanocomposites reached 87.0, 93.2% and 90.1%, respectively, while for ZnO and MnFe<sub>2</sub>O<sub>4</sub>

and samples without catalyst only got 90.8%, 90.6%, and 30.1%. This shows that the ZnO and MnFe<sub>2</sub>O<sub>4</sub> present can change the absorption region and increase the material's activity in visible light. The decrease in MB increased with increasing irradiation time. The reduction in MB concentration at 50 minutes of irradiation reached 93.2% of ZMn-2 nanocomposites compared to ZMn-1, ZMn-3 nanocomposites and ZnO and MnFe<sub>2</sub>O<sub>4</sub> nanoparticles. The best photocatalytic activity was obtained when using ZMn-2 as a catalyst. The photocatalytic degradation reactions (Lee et al., 2016).



### The pH points zero charge (pHpzc)

The pH of the solution is an essential parameter in photocatalytic degradation because the surface charge of the catalyst is affected by the pH of the solution. The type of pollutant and the pH point zero charges (pHpzc) are the main factors determining the optimum pH. The state of pH point zero charges (pHpzc) is a condition when the surface is neutrally charged, which is the point of intersection between the initial pH curve and the final pH curve. To understand the degree of photocatalysis at a given pH, it is essential to determine the isoelectric point or point of zero of the nanocomposites. The pHpzc data estimate the

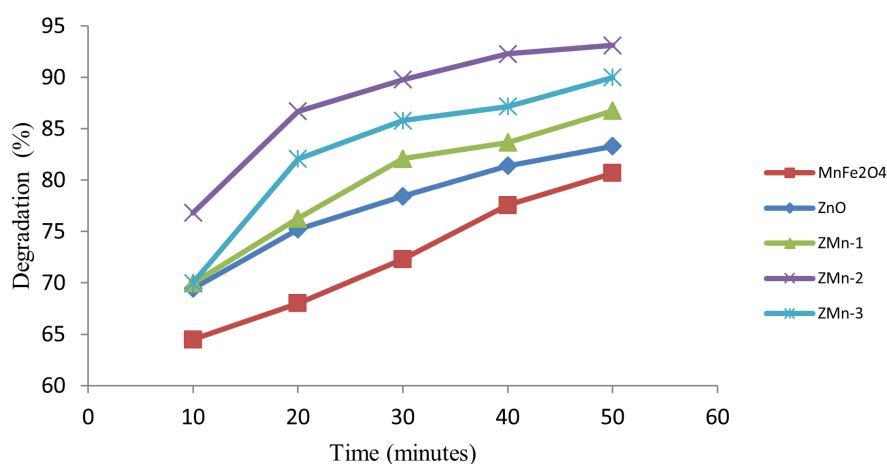


Figure 4. Effect of irradiation time on MB degradation

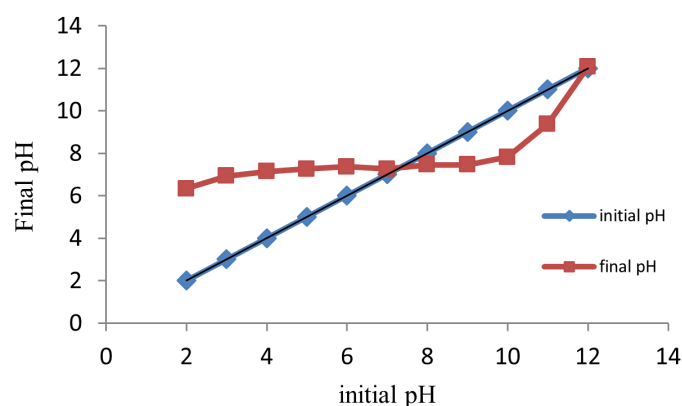


Figure 5. Initial pH to final pH

appropriate pH conditions for the photodegradation process. At low pH,  $H^+$  ions prefer to be on the material's surface than in solution so that the character of  $ZnO/MnFe_2O_4$  is positively charged, which at low pH will easily absorb anions. In contrast, at high pH,  $H^+$  ions prefer to be in solution than in the material, so  $ZnO/MnFe_2O_4$  surface is negatively charged, which at high pH will easily absorb cations (Kulkarni et al., 2017).

Based on Figure 5, a  $pH_{pzc}$  of 7.8 is obtained, which indicates that  $ZnO/MnFe_2O_4$  has a negatively charged pH so that it will quickly absorb the MB dye, which is a cation dye. The results of the  $pH_{pzc}$  nanocomposite  $ZnO/MnFe_2O_4$  obtained, the pH trajectory of methylene blue is below  $pH_{pzc}$  so that, at that pH,  $ZnO/MnFe_2O_4$  will be negatively charged, and it will be easier to absorb methylene blue which includes cation dyes. The  $pH_{pzc}$  value is used to determine suitable pH for effective photocatalytic degradation process. pH optimum depends on the type of pollutant and  $pH_{pzc}$ . For

anion dyes especially methyl orange a pH value of 5.2 was obtained (Hariani et al., 2022). This shows that cation dyes have a pH value  $>7$  which is alkaline (-) while for anion dyes the pH value is  $<7$  which acidic (+).

#### Effect of solution pH

Figure 6 shows the effect of the pH of the solution on the decrease in MB levels. At the pH of the solution =  $pH_{pzc}$ , the  $ZnO/MnFe_2O_4$  photocatalyst nanocomposite is negatively charged. At the same time, MB is a cationic dye and is positively charged when dissolved in water, so there is an attraction between positive and negative ions. When the pH value of the MB solution increased, the degradation increased at pH 4-8, reaching 96% degradation. Under acidic and neutral conditions, both the catalyst surface and MB are positively charged, resulting in repulsion and reducing photocatalytic activity because they cannot provide hydroxyl groups to form hydroxyl

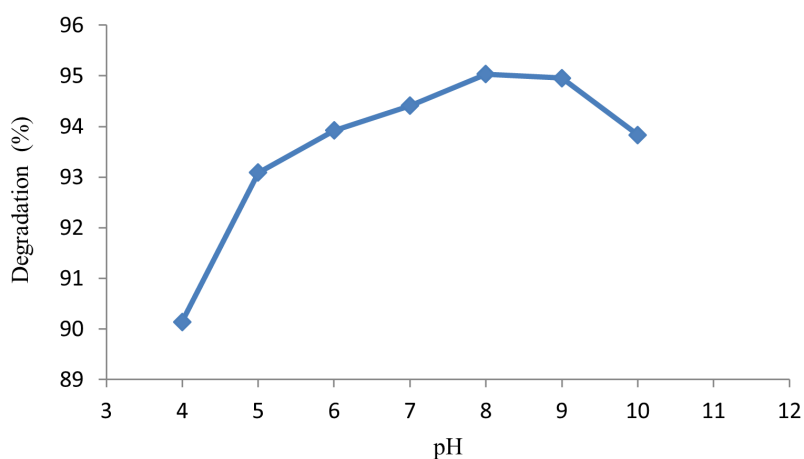


Figure 6. Effect of solution pH on MB degradation

radicals (Kulkarni et al., 2017). On the other hand, the opposite charge on the surface of the catalyst and MB under alkaline conditions creates an attractive force so that the degradation of MB increases.

### Effect of initial dye concentration

Effect of initial MB dye concentration on photocatalytic degradation by varying the concentration of MB 10, 20, 30, 40 and 50 ppm with a catalyst dose of 20 mg under visible light for 50 minutes with a pH of 8. Figure 7 shows that the dye concentration strongly influences the degradation. Initial and decreased from 93.2% to 76.81% with an increase in dye concentration from 10-50 ppm.

The catalyst surface that is open to electron-hole pairs that will produce hydroxyl radicals affects the rate of degradation. In this instance, the catalyst concentration is maintained,

maintaining the same number of hydroxyl radicals while increasing the dye concentration. As a result, the amount of hydroxyl radicals attacking the dye molecules declines, which lowers the rate of degradation.

### Effect of catalyst dose

By changing the  $\text{ZnO/MnFe}_2\text{O}_4$  catalyst amount from 5 to 25 mg over the course of 30 minutes while maintaining a dye concentration of 50 ppm, the effect of catalyst dose on MB photodegradation was examined (Figure 8). Catalyst load rose along with the rate constant. However, there are two areas that may use work. The rise in the quantity of active radicals on the photocatalyst's surface was what caused the rate constant to increase as ZnO concentration was increased.

Due to the rise in hydroxyl radicals, more dye molecules are destroyed as a result. Effect

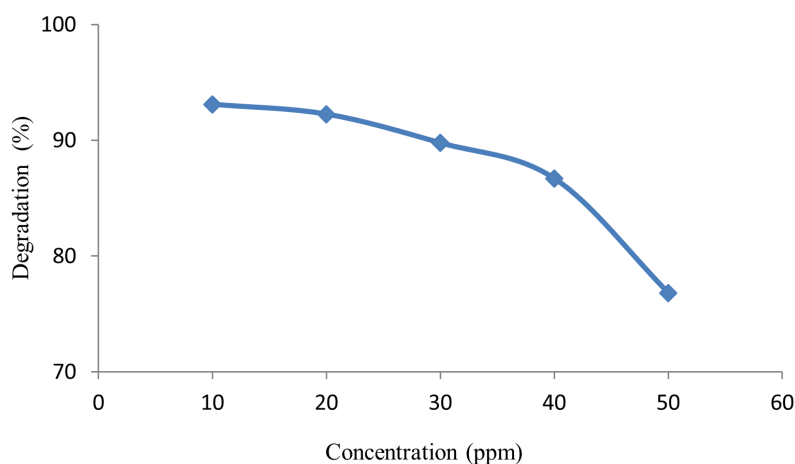


Figure 7. Effect of MB initial concentration on the dye degradation

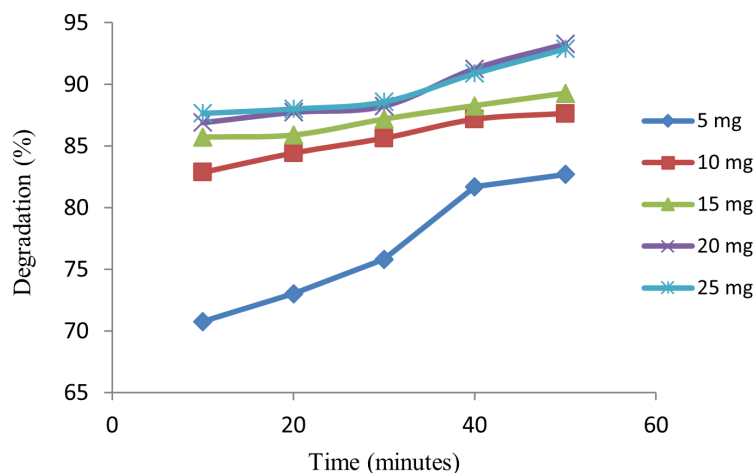


Figure 8. Effect of catalyst dose and irradiation time on MB degradation

of catalyst dose on MB photodegradation caused by changing the catalyst concentration of ZnO/MnFe<sub>2</sub>O<sub>4</sub>.

Increasing the catalyst dose, however, also makes the solution turbid and reduces visible light penetration because it scatters lighter. This component results in a small increase in the rate constant with increasing catalyst dose because it is present at higher catalyst doses (over 1 g). To prevent the catalyst from being used excessively, this was done. This nanocomposite is suggested as a catalyst to decompose dyestuffs in wastewater so that environmental issues brought on by dye wastewater can be addressed due to its strong photocatalytic activity and good stability.

## CONCLUSIONS

ZnO/MnFe<sub>2</sub>O<sub>4</sub> photocatalyst nanocomposites with different compositions from ZnO have been synthesized by the co-precipitation method. From the results of the XRD analysis, the ZnO phase in the nanocomposite shows the hexagonal wurtzite phase while MnFe<sub>2</sub>O<sub>4</sub> shows the cubic spinel phase. The resulting nanocomposite was applied to the degradation of methylene blue dye and the results showed photocatalytic activity of ZnO/MnFe<sub>2</sub>O<sub>4</sub> with a mole ratio of 2:0.1 under visible light after 50 minutes at a dose of 20 mg of the photocatalyst. This shows that the high photocatalytic activity of ZnO/MnFe<sub>2</sub>O<sub>4</sub> is 93.2% and has good stability. This photocatalyst is promising in removing dye pollutants from wastewater and can be used for subsequent applications.

## Acknowledgements

The research/publication of this article was funded by DIPA of Public Service Agency of Universitas Sriwijaya 2021. SP DIPA-023.17.2.677515 /2021, on November 23, 2020. In accordance with the Rector's Decree Number: 0014/ UN9/ SK.LP2M.PT/2021, on Mei 25, 2021. The authors also thank the Central Laboratory of Environmental Research (PPLH) Universitas Sriwijaya and the Postgraduate Integrated Research Laboratory of Universitas Sriwijaya for their laboratory support.

## REFERENCES

1. Agustina T. E., Melwita E., Bahrin D., Gayatri R and Purwaningtyas I.F. 2020. Synthesis of nano-photocatalyst ZnO-natural zeolite to degrade procion red. *International Journal of Technology*, 11(3), 472–481.
2. Boutra B., Guy N., Ozacar M. and Trari M. 2020. Magnetically separable MnFe<sub>2</sub>O<sub>4</sub>/TA/ZnO nanocomposites for photocatalytic degradation of Congo Red under visible light. *Journal of Magnetism and Magnetic Materials*, 497, 165994.
3. Chandel N., Sharma K., Audhaik A., Raizada P., Hosseini-Bandegharai A., Thakur V.K. and Singh P. 2020. Magnetically separable ZnO/ZnFe<sub>2</sub>O<sub>4</sub> and ZnO/CoFe<sub>2</sub>O<sub>4</sub> photocatalysts supported onto nitrogen doped graphene for photocatalytic degradation of toxic dyes. *Arabian Journal of Chemistry*, 13(2), 4324–4340.
4. Długosz O., Szostak K., Krupinski M. and Banach M. 2020. Synthesis of Fe<sub>3</sub>O<sub>4</sub>/ZnO nanoparticles and their application for the photodegradation of anionic and cationic dyes. *International Journal of Environmental Science and Technology*, 18, 561-574.
5. Gayatri R., Agustina T.E., Bahrin D., Moeksin R. and Gustini. 2020. Preparation and Characterization of ZnO-Zeolite Nanocomposite for Photocatalytic Degradation by Ultraviolet Light. *Journal of Ecological Engineering*, 22(2), 178–186.
6. Gómez-pastora J., Dominguez S., Bringas E., Rivero M.J., Ortiz I. and Dionysiou D.D. 2017. Review and perspectives on the use of magnetic nanophotocatalysts (MNPCs) in water treatment. *Chemical Engineering Journal*, 310, 407–427.
7. Güy N. and Özacar M. 2018. Visible light-induced degradation of indigo carmine over ZnFe<sub>2</sub>O<sub>4</sub>/Tannin/ZnO: Role of tannin as a modifier and its degradation mechanism. *International Journal of Hydrogen Energy*, 43(18), 8779–8793.
8. Hariani P. L., Said M., Salni., Aprianti N. and Naibaho, Y. A. L. R. 2022. High efficient photocatalytic degradation of methyl orange dye in an aqueous solution by CoFe<sub>2</sub>O<sub>4</sub>-SiO<sub>2</sub>-TiO<sub>2</sub> magnetic catalyst. *Journal of Ecological Engineering*, 23(1), 118-128.
9. Kefeni K. K. and Mamba B. B. 2020. Photocatalytic application of spinel ferrite nanoparticles and nanocomposites in wastewater treatment : Review. *Sustainable Materials and Technologies*, 23, 1-18.
10. Kulkarni S. D., Kumbar S.M., Menon S.G., Choudhari K.S. and Santosh C. 2017. Novel magnetically separable Fe<sub>3</sub>O<sub>4</sub>@ZnO core-shell nanocomposite for UV and visible light photocatalysis. *Advanced Science Letters*, 23(3), 1724–1729.

11. Lee K. M., Lai C.W., Ngai K.S. and Juan J.C. 2016. Recent developments of zinc oxide based photocatalyst in water treatment technology: A review. *Water Research*, 88, 428-448.
12. Mano T., Nishimoto S., Kameshima Y. and Miyake M. 2015. Water treatment efficacy of various metal oxide semiconductors for photocatalytic ozonation under UV and visible light irradiation. *Chemical Engineering Journal*, 264, 221–229.
13. Ong C. B., Ng L. Y. and Mohammad A. W. 2018. A review of ZnO nanoparticles as solar photocatalysts: Synthesis, mechanisms and applications. *Renewable and Sustainable Energy Reviews*, 81, 536–551.
14. Rahmayeni., Arief S., Jamarun N., Emriadi. and Stiadi, Y. 2017. Magnetically separable ZnO-Mn-Fe<sub>2</sub>O<sub>4</sub> nanocomposites synthesized in organic-free media for dye degradation under natural sunlight. *Oriental Journal of Chemistry*, 33(6), 2758–2765.
15. Shoueir K., El-Sheshtawy H., Misbah M., El-Hosainy, H., El-Mehasseb I. and El-Kemary M. 2018. Fenton-like nanocatalyst for photodegradation of methylene blue under visible light activated by hybrid green DNSA@Chitosan@MnFe<sub>2</sub>O<sub>4</sub>. *Carbohydrate Polymers*, 97, 17–28.
16. Wang D., Guo Z., Peng Y. and Yuan W. 2015. Visible light induced photocatalytic overall water splitting over micro-SiC driven by the Z-scheme system. *Catalysis Communications*, 61, 53–56.
17. Zhang N., Xie S., Weng B. and Xu Y.J. 2016. Vertically aligned ZnO-Au@CdS core-shell nanorod arrays as an all-solid-state vectorial Z-scheme system for photocatalytic application. *Journal of Materials Chemistry A*, 4(48), 18804–18814.